Journal of Coastal Research	SI 56	1085 - 1089	ICS2009 (Proceedings)	Portugal	ISSN 0749-0258

Water Exchange between the Basins of the German Wadden Sea Studied With a Coupled Matlab-Arcgis Model

J.A. Urbański and A. Herman
Institute of Oceanography
University of Gdańsk
81-378 Gdynia, Poland
email: oceju@univ.gda.pl (J.U.)
oceagah@univ.gda.pl (A.H.)

ABSTRACT

URBAŃSKI, J.A. and HERMAN, A., 2009. Water exchange between the basins of the German Wadden Sea studied with a coupled Matlab-ArcGIS model. Journal of Coastal Research, SI 56 (Proceedings of the 10th International Coastal Symposium), 1085 – 1089. Lisbon, Portugal, ISSN 0749-0258.

In this study the water exchange between the basins of the East Frisian Wadden Sea (Germany) is studied numerically by means of a lumped-parameter model in which the geometry of the basins and channels is reduced to a set of a few parameters. Contrary to advanced, high-resolution hydrodynamic models, the simple model enables to identify cause-and-effect relationships between the geometry of the basins and channels and the asymmetries of the open-sea forcing on the one hand and the features of the water circulation within the system on the other hand. The model, implemented in Matlab, is supplemented with a specially designed ArgGIS toolbox enabling to set up the model, to accurately determine its parameters and visualize the results. Two aspects of the water circulation in the study area are considered in detail. Firstly, it is shown that the nonlinearity of the system due to the changing water level depends on the ratio of the cross-sectional areas of the inlets to the surface areas of the basins (both water-level dependent). The influence of this parameter on the tidal asymmetries in the German Wadden Sea is demonstrated. Secondly, the geometry of the system is shown to have a strong influence on the net volume transport through the tidal divides separating the neighboring basins. The results suggest the existence of stable watershed locations between the basins, close to the locations observed in nature.

ADDITIONAL INDEX WORDS: *tidal inlet, tidal divide, tidal asymmetry, volume transport*

INTRODUCTION

The water exchange in shallow coastal basins is an important factor governing e.g. the transport of nutrients, pollutants or sediments. It can be studied with computationally expensive three-dimensional (3D) models or with simplified, lumped-parameter models that can be (re)configured easily and often give a better insight into cause-and-effect relationships between various processes and phenomena occurring in the system under study. Both approaches have obvious advantages and disadvantages and, although the state-of-the-art 3D models are generally preferred nowadays, the simplified models still may offer valuable insights into the functioning of the coastal hydrodynamics, as we demonstrate in this paper.

The main goal of this work is an analysis of two aspects of the water circulation in the East Frisian Wadden Sea, both closely related to the geometry of the system. Firstly, the influence of the varying surface areas of the basins in combination with changes of the cross-sectional areas of the inlets upon the tidal asymmetries is investigated. Secondly, relationships between the geometry of the basins and the net volume transport through the boundaries of those basins are analyzed.

METHODS

The objects constituting our model – the basins and channels connecting them – are reduced to a set of parameters describing their geometry (Table 1). The basins are treated as simple water reservoirs with time-varying, spatially uniform water level. There are two types of channels: open-sea–basin (termed 'inlets' further on) and basin–basin ('tidal divides' or 'watersheds'), as shown in Fig.1. Both channel types are treated in the same way, similarly as in VAN DE KREEKE et al. (2008). Driven by the prescribed open-sea water levels at the entrances to the inlets, a system of continuity and 1D momentum equations is solved, producing time series of water elevations in the basins and current speeds through the channels.

A coupled Matlab-ArcGIS tool was designed that allows for a straightforward model configuration, performing the calculations and visualizing the results. The modelling procedure consists of three steps. Firstly, based on the bathymetric data of the region under study, the building blocks of the model (the boundaries of the basins and channels, their bathymetric curves etc.) are set up with a specially developed ESRI ArcGIS toolbox. Secondly, these data are passed on to a compiled Matlab programme that builds a suitable system of ordinary differential equations (ODEs), solves it numerically and passes the results back to ArcGIS. Finally, the results can be analyzed and visualized with the standard ArcGIS tools. The details of the ArcGIS and Matlab parts of the modelling system are described below.

The lumped-parameter circulation model

The equations of the lumped-parameter model have been formulated by HERMAN (2007) and, in a more general form, by HERMAN (2008). The Graphical User's Interface (GUI), stand-alone version of the model, called SeCoTide (Semi-Connected

Table 1: Parameters describing the geometry of basins and channels considered in the model.

Basins	
$A_{b,i}(z)$	surface area
Channels: open-sea–basin ('c') and basin–basin ('w')	
$A_{c,i}(z)$, $A_{w,i}(z)$	cross-sectional area
$h_{c,i}(z)$, $h_{w,i}(z)$	mean water depth
$L_{c,i}$, $L_{w,i}$	channel length
$\delta_{c,i}$, $\delta_{w,i}$	head-loss damping coefficients

Tidal Inlets), is available online and proved capable of reproducing the main features of water circulation between the basins of the East Frisian Wadden Sea (HERMAN, 2007). Below, only a short description of the governing equations is given; more details concerning the underlying assumptions, limitations and features of the model can be found in the cited papers.

The continuity equation for the i-th of the N basins is formulated in terms of the rate of change (denoted with a prime) of the excess volume of that basin, $V_i \equiv \int_0^{\xi_i} A_{b,i}(z)\mathrm{d}z$:

$$V_i{}' = A_{c,i}u_{c,i} + A_{w,i-1}u_{w,i-1} - A_{w,i}u_{w,i}\,, \qquad (1)$$

where ξ_i denotes the water level in the i-th basin, $u_{c,i}$ – the flow velocity through the inlet connecting that basin to the open sea and $u_{w,i}$ – the flow velocity through the watershed between the basin i and i+1 (see Table 1 for the meaning of the remaining symbols).

The flow through the channels is driven by the along-channel water-level gradient (assumed uniform) and damped by friction:

$$u_{c,i}{}' = \frac{g}{L_{c,i}}\left(\xi_{0,i} - \xi_i\right) - \gamma_{c,i}\left|u_{c,i}\right|u_{c,i}\,, \qquad (2.1)$$

$$u_{w,i}{}' = \frac{g}{L_{w,i}}\left(\xi_i - \xi_{i+1}\right) - \gamma_{w,i}\left|u_{w,i}\right|u_{w,i}\,, \qquad (2.2)$$

with g and $\xi_{0,i}$ denoting the acceleration due to gravity and the open-sea water level at the entrance to the i-th inlet, respectively. The last terms in (2.1) and (2.2) combine the quadratic friction and the nonlinear advection terms (head-loss damping related to the geometry of the channel mouth, see MAAS, 1997, for details):

$$\gamma_{c,i} = gn^2 h_{c,i}^{-4/3} + \delta_{c,i} \quad \text{and} \quad \gamma_{w,i} = gn^2 h_{w,i}^{-4/3} + \delta_{w,i}\,, \qquad (3)$$

where n=0.02 m$^{-1/3}$s denotes the Manning friction factor, assumed constant, and the values of the damping coefficients $\delta_{c,i}$, $\delta_{w,i}$ can be adjusted to the geometry of the individual channels. Contrary to SeCoTide (HERMAN, 2008), where explicit functions have to be provided for the water-level dependent parameters, in the present model the values of $A_{b,i}(z)$, $A_{c,i}(z)$ etc. are interpolated from the lists of values provided from the ArcGIS part of the modeling system, as described below.

The ODE system of 3N–1 equations (1), (2.1), (2.2) is transformed into a matrix form and solved with an efficient multistep solver available in Matlab (SHAMPINE and REICHELT, 1997).

The GIS part of the model

A new ArcToolbox containing four tools was created. Three tools were designed for preprocessing data before sending it to the Matlab model and one for postprocessing the output model data for animation performed in ArcGIS using the animation toolbar. The first tool calculates the surface areas of the basins $A_{b,i}(z)$ for all possible sea levels using the digital elevation model (DEM) of the area and the layer of delineated basins. The second and third tools are used for determination of the channels' parameters. They calculate the mean water depths $h_{c,i}(z)$, $h_{w,i}(z)$ and the cross-sectional areas $A_{c,i}(z)$, $A_{w,i}(z)$ as functions of all possible sea levels using the DEM and the channels transects. The output of these tools is in DBF table format and can be easy imported into the Matlab model. The last tool converts the Matlab output tables to a vector layer of polygons with the same depth range for each time step of the model simulation. This vector layer is then used to create a time layer animation which can be supplemented with figures showing how selected variables change with time.

MODEL SETUP

After the boundaries of the basins, the location of the channels and the parameters describing their geometry by varying water levels have been established in ArcGIS, the model has been run with a number of different boundary conditions, both realistic and artificial, in order to test its performance and sensitiveness to the changes of the parameters. Whereas measured water level time series from a number of tidal stations in the study area are readily available, the current measurements that would be representative for longer time periods are scarce. This is even more true if the medium- and long-term volume transport through the inlets and

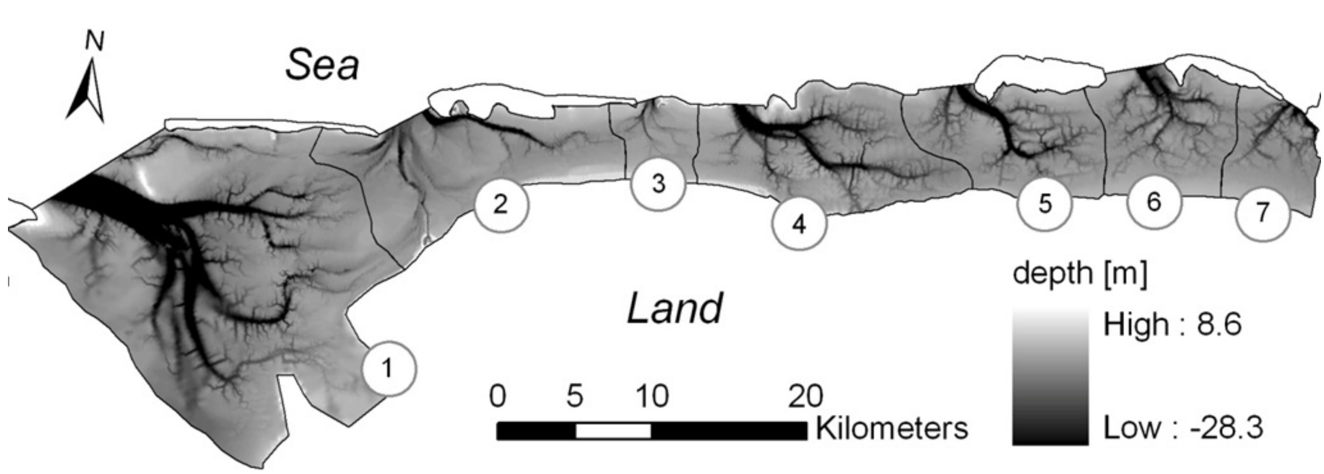

Figure 1. Bottom topography of the study area and the location of the boundaries of the seven basins analyzed.

watersheds is considered, since the locally measured current speeds are generally not representative for the total flow through tidal inlets. Hence, at present numerical modeling is an irreplaceable source of information considering phenomena related to the water and sediment exchange between the tidal basins. In HERMAN (2007) the results of the lumped-parameter model run for the three westernmost East Frisian basins (No.1–3 in Fig.1) have been successfully verified against the results of the high-resolution hydrodynamic model Delft3D (see also HERMAN et al., 2007). Importantly, both with realistic and simplified open-boundary conditions the simple model produced values of the net volume transport through the basins' boundaries consistent with those obtained with Delft3D. In the present work, the values of those model parameters that couldn't be obtained directly from the DEM of the area with the ArcGIS toolbox (e.g. the $\delta_{c,i}$, $\delta_{w,i}$ coefficients) were set first for basins 1–3 to minimize the differences between the Delft3D and the lumped-parameter model results. Then, based on geometric similarity arguments (see next section), the analogous parameters for the remaining basins were estimated.

Below the results of the model forced with the M_2 tide are shown, as they provide a better illustration of the processes discussed here than the 'realistic' forcing. The amplitudes and phases of the M_2 tidal component at the entrances to the subsequent basins were established based on a harmonic analysis of the results of a large-scale numerical model.

ANALYSIS AND DISCUSSION

Nonlinearities due to the geometry of the system

Since the pioneering works of ESCOFFIER (1940) and O'BRIEN (1969), morphological studies of various tidal basins around the world revealed the existence of some universal constraints concerning the relative dimensions of the basin/inlet systems and the quantities characterizing their hydrodynamics (e.g. equilibrium current velocities through the inlets). For the German Wadden Sea, a number of such empirical relationships, e.g. linking the basin surface area with the tidal prism, were formulated by SCHROEDER et al. (1994) and NIEMEYER et al. (1995). The majority of those relationships is limited to the values of the analyzed parameters at the mean water level z=0. However, as demonstrated by MAAS (1997) and STANEV et al. (2003a), the dependence of the basins' surface areas on the water level introduces an additional nonlinearity (apart from the friction) to the system, thus influencing the asymmetry of the tidal curves and the flow velocities through the inlets. Assuming a linear dependence of $A_{b,i}(z)$ on the water level, STANEV et al. (2003a) performed a detailed analysis of the influence of drying and flooding of the tidal flats on the generation of higher-order harmonics in the East-Frisian basins. However, it can be demonstrated easily that it is the $A_c(\xi)/A_b(\xi)$ ratio, not $A_b(\xi)$ alone, that determines the nonlinear behavior of the system. To illustrate this, let us set $A_{b,i}(\xi)=A_{b0,i}\alpha_{b,i}(\xi)$ and $A_{c,i}(\xi)=A_{c0,i}\alpha_{c,i}(\xi)$, where $A_{b0,i}$ and $A_{c0,i}$ denote the respective parameters at ξ=0 and $\alpha_{b,i}(\xi)$, $\alpha_{c,i}(\xi)$ describe their changes due to changing water level. Let us further introduce the following variables:

$$\upsilon_{c,i} = u_{c,i} A_{c,i} / A_{b,i} \quad \text{and} \quad \hat{\upsilon}_{w,i} = u_{w,i} A_{w,i} / A_{b,i} \tag{4}$$

and the set of parameters:

$$\sigma^2_{c,i} = \frac{g A_{c0,i}}{L_{c,i} A_{b0,i}}, \quad \alpha_i = \frac{\alpha_{c,i}}{\alpha_{b,i}} \quad \text{and} \quad \beta_i = \frac{\gamma_{c,i} A_{b0,i}}{A_{c0,i}}. \tag{5}$$

As can be seen from (4), $\upsilon_{c,i}$ and $\hat{\upsilon}_{w,i}$ represent the rate of change of the water level in the i-th basin due to the flow to/from the open sea and to/from its right neighbor. After some straightforward algebra equation (1) can be transformed into:

$$\xi_i' = \upsilon_{c,i} + \hat{\upsilon}_{w,i-1} A_{b,i-1} / A_{b,i} - \hat{\upsilon}_{w,i}. \tag{6}$$

In (5) $\sigma_{c,i}$ corresponds to the Helmholtz frequency defined traditionally for single basins with vertical walls. Using (4), (5) and (6) the momentum equations (2.1) can be transformed into:

$$\upsilon_{c,i}' = \sigma^2_{c,i} \alpha_i \left(\xi_{0,i} - \xi_i\right) - \frac{\beta_i}{\alpha_i} \left|\upsilon_{c,i}\right| \upsilon_{c,i} + \frac{1}{\alpha_i} \frac{d\alpha_i}{d\xi} \upsilon_{c,i} \xi_i' \tag{7}$$

(analogous equations can be formulated for (2.2); see also HERMAN, 2008). As shown in Fig.2a, $\alpha_i(\xi)$ has a similar form for all basins under study – with an exception of the smallest and shallowest basin of Baltrum (No.3). For the remaining basins $\alpha_i(\xi)$ varies only slightly within the tidal range. To a good approximation $\alpha_i(\xi)$=1 and dα_i/dξ =0 for $\xi \geq 0$. Also, for $\xi<0$ we have dα_i/dξ<0. Consequently, at low water levels the last term in (7) acts to increase/reduce the apparent friction during inflow/outflow. If we disregard the inter-basin exchange for a moment ($\hat{\upsilon}_{w,i}$=0), then the sum of the nonlinear terms in (7) becomes:

$$\frac{1}{\alpha_i} \left(-\beta_i \,\mathrm{sgn}(\upsilon_{c,i}) + \frac{d\alpha_i}{d\xi} \right) \upsilon^2_{c,i} = F_{n,i} \upsilon^2_{c,i}. \tag{8}$$

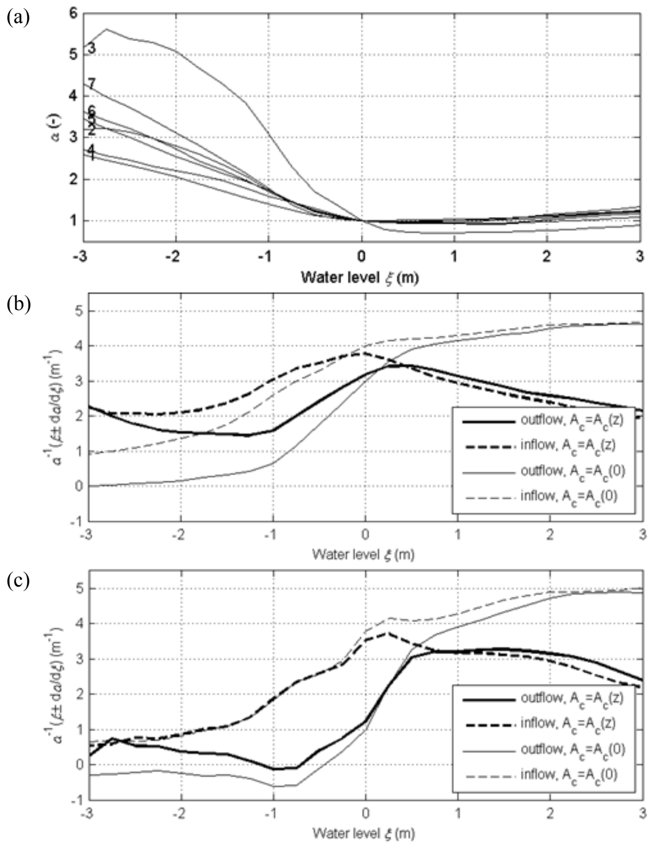

Figure 2. (a): parameter $\alpha_i(\xi)$, defined in (5), for basins 1–7, numbered as in Fig. 1. (b,c): coefficients of the total nonlinear term in equation (7) during inflow ($-F_{n,i}$, dashed lines) and outflow ($F_{n,i}$, continuous lines) for basin No. 2 (b) and 3 (c). In (b) and (c), values corresponding to $\alpha_i(\xi)=1/\alpha_{b,i}(\xi)$ (channels with constant cross-sectional areas) are shown with thin lines and those corresponding to $\alpha_i(\xi)=\alpha_{c,i}(\xi)/\alpha_{b,i}(\xi)$ – with thick lines.

In Fig.2b,c $F_{n,i}$ is shown for two chosen basins for both inflow ($\upsilon_{c,i}>0$) and outflow ($\upsilon_{c,i}<0$) situation and calculated in two versions: assuming $A_{c,i}(z)=A_{c0,i}$ (or, equivalently, $\alpha_{c,i}\equiv 1$), as in STANEV et al. (2003a), and $A_{c,i}(z)$ estimated from the DEM. At positive water levels, higher than ~0.5m, the difference between the two methods becomes significant; if variability of $A_{c,i}$ is taken into account, the magnitude of the nonlinear term begins to decrease with increasing water level, whereas constant $A_{c,i}$ results in monotonically increasing $F_{n,i}$ in the whole range of water levels. At negative water levels the influence of variable $A_{c,i}$ is for all basins more pronounced during the ebb than during the flood current. Generally, within the range of the M_2 tide analyzed here, the difference between the $F_{n,i}$ values calculated with the two methods may reach 30–40% and it is not surprising that it has a noticeable influence on the simulated currents, as shown in Fig.3. Although the differences in water levels do not exceed 10 cm (and are highest shortly before the high and low water), the current speeds change by up to 20 cm/s. In the smaller inlets (e.g. No.3 shown in Fig.3) variable $A_{c,i}(z)$ leads to weaker flood currents, thus contributing to the ebb-dominance of those inlets.

Net volume transport through the tidal divides

Another interesting aspect of water circulation in the analyzed system of semi-connected basins, often disregarded in numerical studies (e.g. STANEV et al, 2003a,b), is a non-zero net volume transport through the tidal divides. Although the current speeds and the cross-sectional areas of watersheds are much smaller than those of the inlets, and some watersheds fall almost completely dry at low water (see a snapshot of the area in Fig.5 for an example), the flow through the tidal divides contributes substantially to the overall water balance of the basins. As shown in HERMAN (2007) the net volume transport through the left and right tidal divides of the basin of Norderney due to the M_2 forcing equals $16\cdot 10^6$ and $4.8\cdot 10^6$ m^3/tide, respectively (results of the hydrodynamic model Delft3D). With realistic model forcing the values are typically much higher. Here we investigate the issue in more detail for all seven basins, concentrating on two quantities that have a crucial influence not only on the hydrodynamics, but on the morphodynamics of the system as well: the maximum current speeds through the tidal divides, $u_{w,max}$, and the total volume transport V_{tot}. The amount of sediment suspended in the water column and the conditions favorable for deposition/erosion both depend on $u_{w,max}$ (e.g. RIBBERINK, 1998). In the present study, calculations with the 'classical' sediment-transport formulae (USACE, 2002) showed that the critical value of the Shields parameter is never exceeded in the model setting considered – which means that the bed-load sediment transport through the watersheds is insignificant. Hence, if a constant suspended-sediment concentration in a water column is assumed (PEJRUP, 1988; VINTHER et al., 2004), V_{tot} is a direct measure of the cumulative sediment transport through tidal divides.

To investigate the relationships between the relative sizes of the basins and the sign and amplitude of V_{tot}, we performed a following analysis: first, for a given pair of basins, i and i+1, the approximate location of the watershed was expressed as a number $p_i\in(0,1)$ describing its position relative to the west end of the respective island. Then, by varying p_i, the watershed was 'moved' along the island from its true position, which is equivalent to increasing/decreasing the relative surface areas of the basins. An assumption was made that all dimensions of the basins and channels changed together with the changes of surface areas, in such a way that the empirical relationships formulated for the East Frisian Wadden Sea were satisfied at all times – i.e. the changes are assumed to be slow enough so that the system can steadily adjust to them. Considering slow sediment transport rates through the watersheds it is a reasonable assumption.

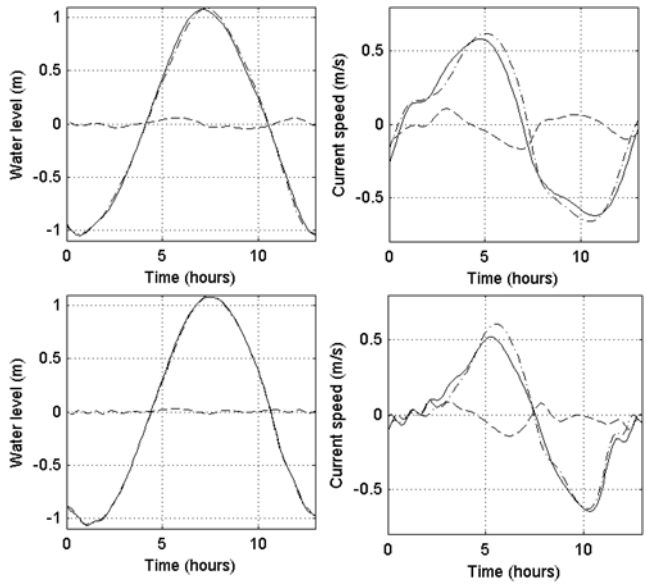

Figure 3. Water levels (left) and current speeds (right) in basin No.2 (above) and No.3 (below). Dash-dotted lines: simulations with $A_{c,i}(z)=A_{c0,i}$, continuous lines: simulations with variable $A_{c,i}(z)$, dashed lines: difference between the two time series. Positive current speeds mean flow into the basin.

As an example of the results of that numerical experiment, the net volume transport between basins No.3 and 4 as a function of p is shown in Fig.4. The most important result is that for some $p=p_s$ (in that case equal 0.58) V_{tot} changes sign from positive to negative. Hence, this watershed location can be regarded as a stable equilibrium in the sense that the watershed will tend to shift to the right (left) if $p<p_s$ ($p>p_s$), in both cases back towards the equilibrium position. As can be seen in Fig.1 and 5, the actual position of the discussed tidal divide is very close to this theoretically estimated equilibrium. Generally, for larger basins p_s is also larger, usually between 0.6 and 0.8 – as our results suggest, this is related to the fact that for larger basins, separated from the sea by longer islands, the phase shift of the tidal signal at the entrance to the subsequent inlets, $\Delta\phi$, is larger as well. HERMAN (2007) shown that V_{tot} increases with increasing $\Delta\phi$. Remarkably, independently on the basins size, the maximum current speeds $u_{w,max}$ in vicinity of the stable equilibrium are up to 50% lower than those obtained for p much lower or much higher than p_s (not shown).

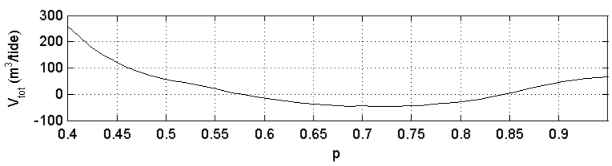

Figure 4. Total volume transport through the watershed between basins No.3 and 4, for varied relative sizes of those basins, expressed in terms of the watershed location p (see text for more detailed description).

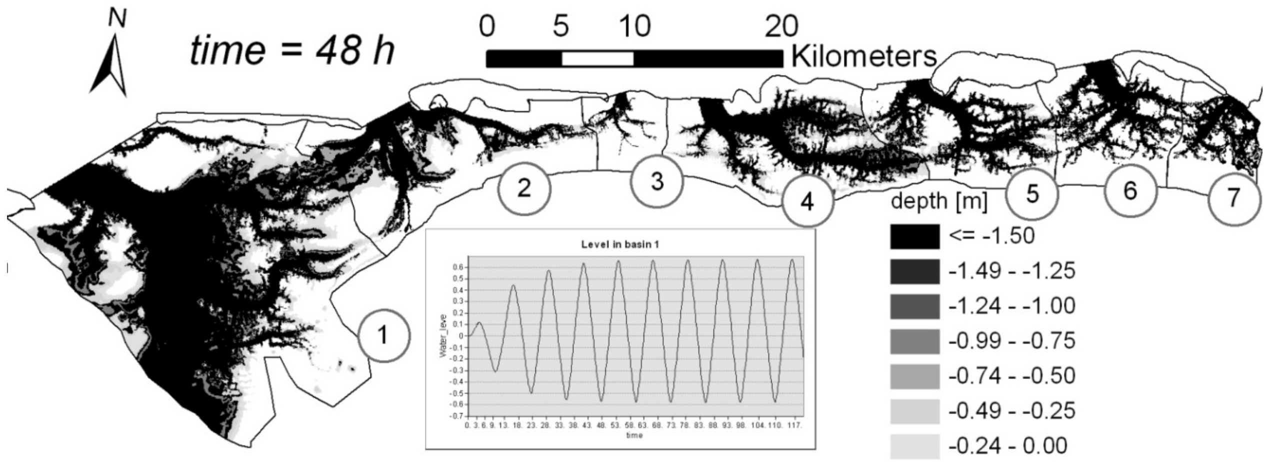

Figure 5. Selected frame of the animation performed in ArcGIS for the analysis purpose.

SUMMARY AND OUTLOOK

When interpreting the results presented in this paper it must be remembered that they have been obtained with a very simple model and thus their accuracy is certainly limited due to a number of simplifying assumptions made by the model formulation. On the other hand, the results reveal some features of the water circulation in the tidal basins that would be very difficult to identify in (or extracted from) the results of three-dimensional hydrodynamic models. In particular, the methods of the dynamic systems, for practical reasons applicable only to systems with a limited number of dimensions, can be used without problems to study the behavior of simplified models. In this respect it seems reasonable to regard the lumped-parameter model presented here as a useful tool supplementary to the high-resolution state-of-the-art models.

The results of modeling can be analyzed in ArcGIS in many ways. One of them is animation of spatial changes in time using complex visualization configuration with maps and time series plots (Fig.5) that provide valuable insights into the spatio-temporal changes of water levels and currents in the study area. In a subsequent study, the present model will be extended for more general topologies of basins and channels. Together with extensive visualization and analysis possibilities of ArcGIS, this will make the coupled Matlab-ArcGIS model a flexible tool applicable to a much wider range of problems than those presented in this paper.

LITERATURE CITED

ESCOFFIER, F.F., 1940. The stability of tidal inlets. *Shore and Beach*, 8, 114-115.

HERMAN, A., 2007. Numerical modelling of water transport processes in partially-connected tidal basins. *Coastal Engineering*, 54, 297-320.

HERMAN, A., 2008. *SeCoTide User's Guide, version 0.9*. Online at http://www.ocean.univ.gda.pl/~herman/SeCoTide/SeCoTide.htm, 33p.

HERMAN, A.; KAISER, R., and NIEMEYER, H.D., 2007. Modelling of a medium-term dynamics in a shallow tidal sea, based on combined physical and neural network methods. *Ocean Modelling*, 17, 277-299.

MAAS, L., 1997. On the nonlinear Helmholtz response of almost-enclosed tidal basins with sloping bottoms. *Journal of Fluid Mechanics*, 349, 361-380.

NIEMEYER, H.D.; GOLDENBOGEN, R.; SCHROEDER, E., and KUNZ, H., 1995. Investigations into the morphodynamics of the Wadden Sea in the research project WADE. *Die Küste*, 57, 65-94 (in German).

O'BRIEN, M.P., 1969. Equilibrium flow areas of inlets on sandy coasts. *Journal of Waterway, Port, Coastal and Ocean Engineering*, 95, 43-52.

PEJRUP, M., 1988. Suspended sediment transport across a tidal flat. *Marine Geology*, 82, 187-198.

RIBBERINK, J.S., 1998. Bed-load transport for steady flows and unsteady oscillatory flows. *Coastal Engineering*, 34, 59-82.

SCHROEDER, E.; GOLDENBOGEN, R., and KUNZ, H, 1994. Parameterization for conceptual morphodynamic models of Wadden Sea areas. *24th International Conference on Coastal Engineering*, Kobe, Japan, 3251-3265.

SHAMPINE, L.F. and REICHELT, M.W., 1997. The Matlab ODE suite. *SIAM Journal of Scientific Computing*, 18, 1-22.

STANEV, E.V.; FLÖSER, G., and WOLFF, J.-O., 2003a. First- and higher-order dynamical controls on water exchanges between tidal basins and the open ocean. A case study for the East Frisian Wadden Sea. *Ocean Dynamics*, 53, 146-165.

STANEV, E.V.; WOLFF, J.-O.; BURCHARD, H.; BOLDING, K., and FLÖSER, G., 2003b. On the circulation in the East Frisian Wadden Sea: numerical modeling and data analysis. *Ocean Dynamics*, 53, 27-51.

U.S. Army Corps of Engineers (USACE), 2002. Coastal Engineering Manual. Part III, Chapter 6: Sediment transport outside the surf zone. *USACE Report EM 1110-2-1100*, 72p.

VAN DE KREEKE, J.; BROUWER, R.L.; ZITMAN, T.J., and SCHUTTELAARS, H.M., 2008. The effect of a topographic high on the morphological stability of a two-inlet bay system. *Coastal Engineering*, 55, 319-332.

VINTHER, N.; CHRISTIANSEN, C.; BARTHOLDY, J.; SØRENSEN, C., and LUND-HANSEN, L.C., 2004. Sediment transport across a tidal divide in the Danish Wadden Sea. *Danish Journal of Geography*, 104, 71-86.

ACKNOWLEDGEMENTS

Part of the work has been done within the project No. BW/1330-5-0265-8 sponsored by the University of Gdansk.